

# Effect of glucose on the optical properties of arterial blood using Mie theory simulations

Neil T. Clancy<sup>a</sup> and Martin J. Leahy<sup>b</sup>  
Department of Physics, University of Limerick, Ireland.

## ABSTRACT

The glucose concentration in arterial plasma has immediate effects on the optical properties of blood-bearing tissue due primarily to the alteration of refractive index mismatch between the scattering particles (red blood cells) and the medium (plasma). The influence of these effects on pulse oximetry is investigated using a numerical model based on Mie theory. The objective is to determine whether or not physiological fluctuations in blood glucose levels could sufficiently vary the optical properties to shift the calibration curve of a commercial pulse oximeter significantly.

**Keywords:** Glucose, pulse-oximetry, Mie theory, scattering particles.

## 1. INTRODUCTION

The effect of varying glucose concentration ( $c_g$ ) in a phantom containing polystyrene microspheres has been studied previously<sup>1</sup>. In the microsphere suspension, the absorption coefficient of the host medium (water) was affected by the addition of the intrinsic glucose absorption coefficient ( $\mu_a^w$ ) and the displacement of water. However, at the wavelengths chiefly of interest in this paper (commercial pulse oximeter wavelengths in the red/infrared), the absorption by water/glucose in plasma is significantly lower than that of haemoglobin (a factor of  $\sim 10^3$ ), the main chromophore in blood in this region. It was found that glucose had a significant influence on the optical properties by altering the refractive index mismatch between the scattering particle and medium. More importantly, dissolving glucose in the suspension reduced the refractive index mismatch between the particle and medium thus reducing the scattering. This is a phenomenon that has already been exploited in optical clearing, where the addition of glucose has been used to achieve greater penetration by light into tissue<sup>2</sup>.

Pulse oximetry is a widely used technique but its accuracy and reliability are affected by physiological conditions different to those under which the instrument was calibrated. This empirical calibration involves *in vivo* measurements on a set of 'healthy' volunteers recording the red to infrared ratio from the device while simultaneously measuring  $\text{SaO}_2$  with a 'gold-standard' instrument such as a co-oximeter. Under typical physiological conditions,  $c_g$  can vary to double its minimum value (preprandial). An error of 1 % in the calibration curve resulting from this effect would be clinically significant, > 3 % would be serious. In this paper, the effect that variations of  $c_g$  in arterial blood plasma has on pulse oximetry is investigated via Mie simulations and a numerical model based on photon diffusion theory.

## 2. THEORY

Mie theory is an exact solution to Maxwell's equations and has been found previously to provide an excellent description of the scattering properties of red blood cells (RBCs)<sup>3</sup>. This theory has been described in depth by Bohren and Huffman<sup>4</sup> and it is this formulation that the computer simulation is based on. The scattering coefficient is calculated from the scattering efficiency and the density of scatterers,  $\rho_s$ .

$$\rho_s = \frac{H}{v_i} \quad (1)$$

Where  $H$  = haematocrit (0.45) and  $v_i$  = mean volume of a RBC ( $90.48 \mu\text{m}^3$ )<sup>5</sup>

---

<sup>a</sup> neil.clancy@ul.ie; phone +35361 202307; <sup>b</sup> martin.leahy@ul.ie; phone +35361 213056

The absorption cross-section of an individual RBC is calculated knowing its absorption efficiency  $Q_a$  (derived from Mie theory) and geometrical cross-section  $A$  (circle of radius equal to the average radius of a RBC, 2.76  $\mu\text{m}$ ):-

$$\sigma_a = Q_a A \quad (2)$$

The bulk coefficient can then be computed knowing the density of absorbers.

$$\Sigma_a = \sigma_a \rho_s \quad (3)$$

Similarly, for scattering

$$\sigma_s = Q_s A \quad (4)$$

$$\Sigma_s = \sigma_s \rho_s \quad (5)$$

$$\Sigma'_s = \Sigma_s (1 - g) \quad (6)$$

where  $g$  is the anisotropy factor and  $\Sigma'_s$  is the reduced scattering coefficient.

Based on an empirical relation used by Tuchin *et al.*<sup>6</sup>, the refractive index was varied according to the following:

$$\eta_{\text{PLASMA}} = \eta_{\text{PLASMA}}^* + 0.1515c_g \quad (7)$$

where  $\eta_{\text{PLASMA}}^*$  is the average refractive index of the plasma<sup>2</sup> as shown in table 1.

Photon diffusion analysis was used to generate theoretical calibration curves based on the bulk optical properties of the medium in question (arterial blood in this case). This has been described in detail previously<sup>7</sup> and has been demonstrated to provide an excellent match to experimentally obtained data<sup>8</sup>. The following equations were used in the case of backscatter detection:

$$\frac{(dI/I)_R}{(dI/I)_{IR}} = \frac{\Sigma'_s K_B(\alpha_R, r)}{\Sigma'_s K_B(\alpha_{IR}, r)} \bullet \left( \frac{\Sigma_{aR}^{\text{art}}}{\Sigma_{aIR}^{\text{art}}} \right) \quad (8)$$

where,

$$K_B(\alpha_n, r) \approx \frac{-r^2}{1 + \alpha_n r} \text{ for } 2\alpha_n r \gg 1$$

and the attenuation coefficient  $\alpha$ ,

$$\alpha = \sqrt{3 \Sigma_a (\Sigma'_s + \Sigma_a)} \quad (9)$$

where  $r$  is the source-detector separation,  $R$  and  $IR$  are the red and infrared wavelengths used respectively and  $\Sigma_{a n}^{\text{art}}$  is the bulk absorption coefficient for arterial blood at a specified wavelength  $n$ .

In the transmission case, the coefficient  $K_B$  is replaced by:

$$K_T(\alpha_n, d) \approx \frac{\alpha_n d - 1}{\alpha_n^2 d} \text{ for } \alpha_n d \gg 1$$

where  $d$  is the thickness of tissue separating the source and detector.

### 3. METHOD

A Matlab implementation was written based on code originally developed by Mätzler<sup>9</sup> that allows for calculation of a spectrum of optical properties from the input parameters (summarised in table 1). Absorption data for haemoglobin using data compiled by Prahl<sup>10</sup> were used.

RBC radius / $\mu\text{m}$	2.76
RBC volume / $\mu\text{m}^3$	90.48
Haematocrit	0.45
$\eta_{\text{RBC}}$	1.4
$\eta_{\text{plasma}}^*$	1.342
Wavelength Range / nm	250 - 1000

Table 1: Input values used in the Mie theory simulations. The values for the dimensions of the RBC are mean values.

The model consists of a homogeneous suspension of scattering spheres (RBCs) in a non-absorbing medium (plasma). The spheres contain haemoglobin at a typical physiological concentration ( $\sim 333 \text{ g l}^{-1}$  per RBC, calculated by dividing the concentration of haemoglobin in whole blood [ $150 \text{ g l}^{-1}$ ] by the number density of RBCs) and absorb light accordingly. The effect of glucose is considered via the implications of its refractive index. The major assumptions here are that the RBCs are spherical, haemoglobin is confined exclusively to the RBCs and glucose is confined exclusively to the plasma. The spherical RBC assumption (actually a biconcave disc) does result in over-estimation of  $g$  compared with experimental results but  $\Sigma_s$  agrees quite well with theory<sup>3</sup>.

The approach used here is to utilise the numerical simulations in Mie theory to estimate the variation in the scattering coefficients of arterial blood at the wavelengths of interest. This variation is then applied to the photon diffusion model via the scattering properties of the arterial blood (Table 2) to investigate how much the calibration curve of a particular pulse oximeter might vary as  $c_g$  is changed from its minimum to maximum value.

#### 4. RESULTS

The bulk optical properties of the ‘model’ arterial blood in the 250 – 1000 nm range for constant  $\text{SaO}_2$  (typical physiological level of 95 %) are presented in figure 1. The visible range is shown to highlight the effect of the strong absorption by the haemoglobin species on the scattering properties.

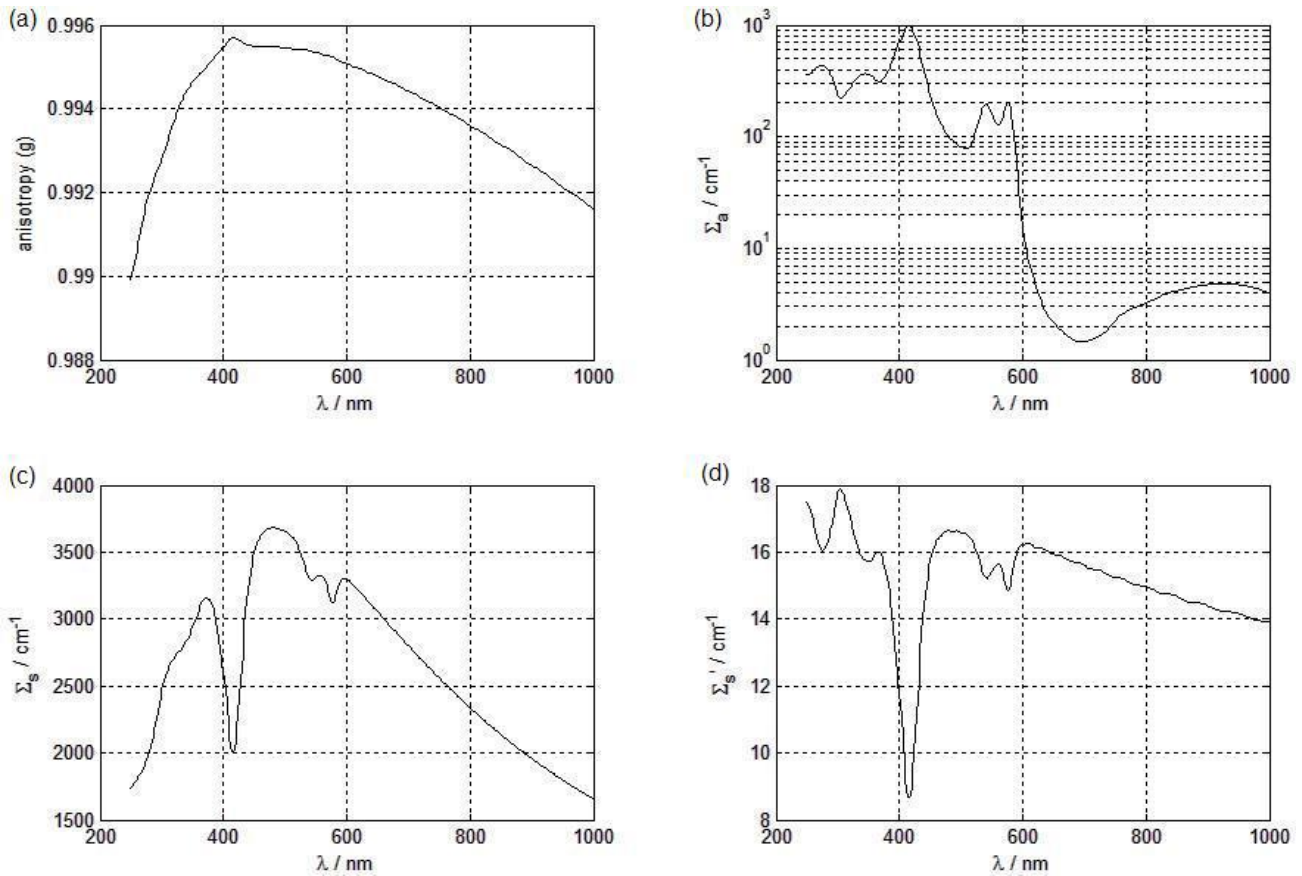


Figure 1: Optical properties of the ‘model’ arterial blood generated by the Mie theory simulation including the anisotropy factor (a), absorption coefficient (b), scattering coefficient (c) and reduced scattering coefficient (d), where  $\Sigma_s' = (1 - g)\Sigma_s$ . All are expressed as a function of wavelength with  $\text{SaO}_2 = 0.95$ ,  $c_g = 90 \text{ mg dl}^{-1}$  and haemoglobin concentration =  $333.33 \text{ mg dl}^{-1}$  per RBC (the influence of the absorption properties of the RBCs due to haemoglobin can be seen clearly in the 250 – 600 nm region).

The effect of varying  $c_g$  is investigated with regard to two pulse oximeter systems (sections 4.1 and 4.2) – the commonly used commercial wavelengths of 660/940 nm (chiefly used in transmission set-ups) and a 675/790 nm pair (developed for use with a reflection probe <sup>8</sup>).

	675 nm		790 nm	
$\Sigma'_s \text{ blood} / \text{cm}^{-1}$	$c_g = 90 \text{ mg dl}^{-1}$ $c_g = 180 \text{ mg dl}^{-1}$		$c_g = 90 \text{ mg dl}^{-1}$ $c_g = 180 \text{ mg dl}^{-1}$	
	25.26	25.54	42.26	42.74
	660 nm		940 nm	
$\Sigma'_s \text{ blood} / \text{cm}^{-1}$	$c_g = 90 \text{ mg dl}^{-1}$ $c_g = 180 \text{ mg dl}^{-1}$		$c_g = 90 \text{ mg dl}^{-1}$ $c_g = 180 \text{ mg dl}^{-1}$	
	25.26	25.54	18.89	19.11

Table 2: Scattering coefficients for arterial blood used in photon diffusion model to generate calibration curves at the lower ( $c_g = 90 \text{ mg dl}^{-1}$ ) and upper ( $c_g = 180 \text{ mg dl}^{-1}$ ) glucose concentration limits.

SaO <sub>2</sub> (%)	Reflection (R/IR)				Transmission (R/IR)			
	Lower limit		Upper limit		Lower limit		Upper limit	
	675/790 nm	660/940 nm	675/790 nm	660/940 nm	675/790 nm	660/940 nm	675/790 nm	660/940 nm
100	0.46	0.48	0.46	0.48	0.47	0.49	0.47	0.49
95	0.62	0.66	0.62	0.66	0.63	0.66	0.63	0.65
90	0.77	0.82	0.77	0.82	0.77	0.81	0.77	0.80
85	0.90	0.97	0.90	0.97	0.89	0.95	0.89	0.94
80	1.01	1.11	1.01	1.11	0.99	1.09	0.99	1.07
75	1.12	1.25	1.11	1.25	1.09	1.21	1.09	1.20
70	1.21	1.38	1.21	1.38	1.18	1.33	1.18	1.32
65	1.30	1.51	1.30	1.51	1.26	1.45	1.25	1.43
60	1.38	1.64	1.38	1.64	1.33	1.56	1.33	1.54
55	1.45	1.77	1.45	1.77	1.39	1.67	1.39	1.65
50	1.52	1.89	1.52	1.89	1.46	1.78	1.45	1.76
45	1.59	2.01	1.58	2.01	1.51	1.89	1.51	1.86
40	1.65	2.14	1.64	2.14	1.57	1.99	1.56	1.97
35	1.70	2.26	1.70	2.26	1.62	2.10	1.61	2.07
30	1.75	2.38	1.75	2.38	1.66	2.20	1.66	2.17
25	1.80	2.51	1.80	2.51	1.70	2.31	1.70	2.28
20	1.85	2.63	1.85	2.63	1.75	2.41	1.74	2.38
15	1.89	2.76	1.89	2.76	1.78	2.52	1.78	2.49
10	1.94	2.89	1.93	2.89	1.82	2.63	1.82	2.60
5	1.99	3.06	1.99	3.06	1.87	2.78	1.87	2.75
0	2.04	3.24	2.04	3.24	1.92	2.94	1.92	2.90

Table 3: Red-to-infrared ratios generated by photon diffusion theory for each wavelength pair in reflection and transmission mode.

#### 4.1 Simulation results for wavelength pair: 675/790 nm

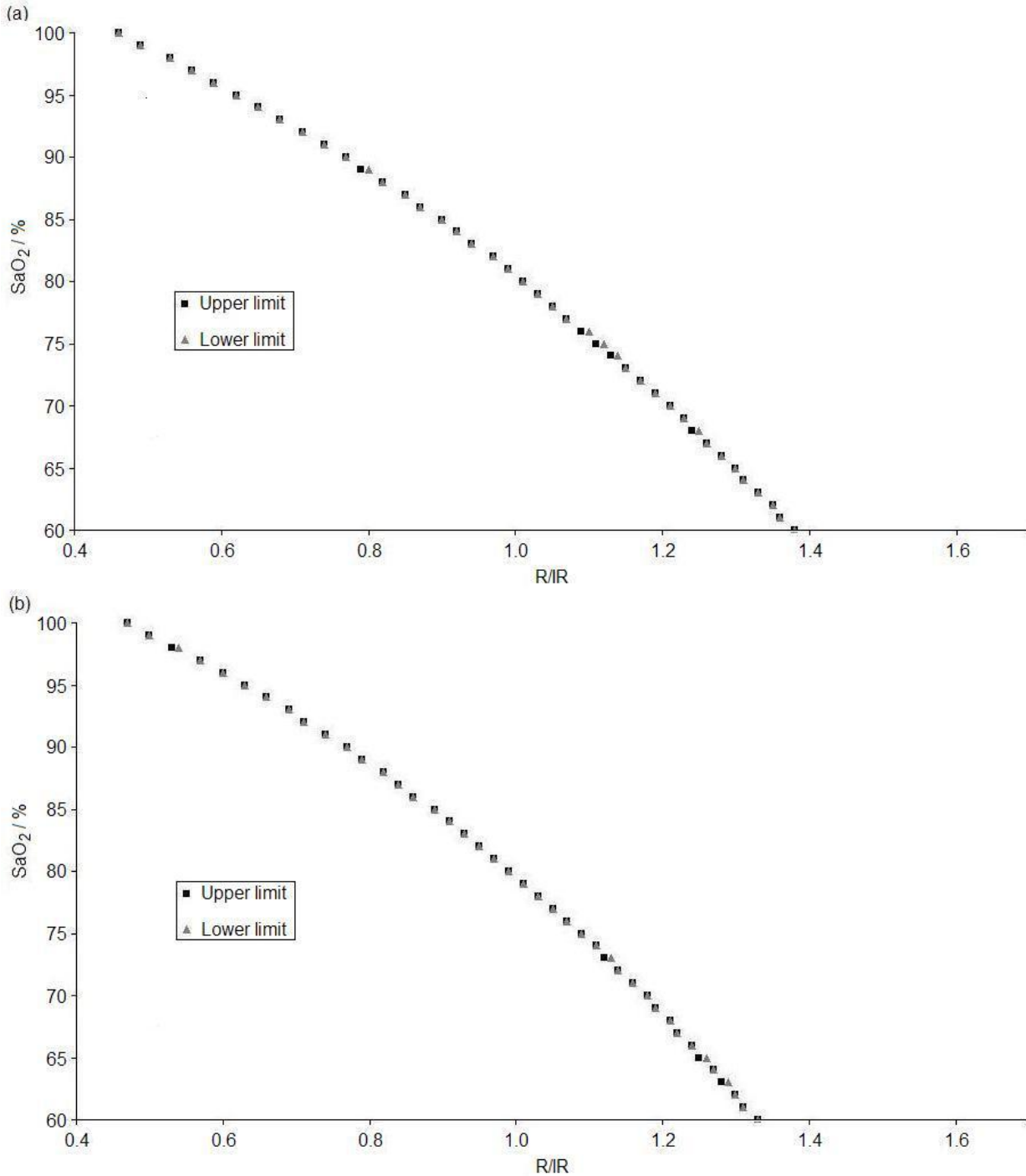


Figure 2: Pulse oximeter calibration curves as calculated by using photon diffusion theory for the 675/790 nm pair in (a) reflection and (b) transmission mode. By using the variations in  $\Sigma_s^{\text{blood}}$  estimated from the Mie simulations, upper and lower limits were calculated for both extremes of the variation. R/IR is the red to infrared ratio of absorption of red to infrared light in the arterial blood.

Across the wavelength range investigated,  $\Sigma_s$  varied on average by 0.3 % (0.32 % at 675 nm and 0.38 % at 790 nm) while  $\Sigma_s'$  varied by 0.57 % (0.57 % at both 675 and 790 nm). This estimated variation in reduced scattering coefficient for arterial blood ( $\Sigma_s^{\text{blood}}$ ) was implemented in the photon diffusion model and resulted in an average shift in the

calibration curve of just 0.13 % in the 'normal' operating conditions ( $70 \% < SpO_2 < 100 \%$ ). Below 70 %  $SpO_2$ , this variation falls to less than 0.08 %.

#### 4.2 Simulation results for wavelength pair: 660/940 nm

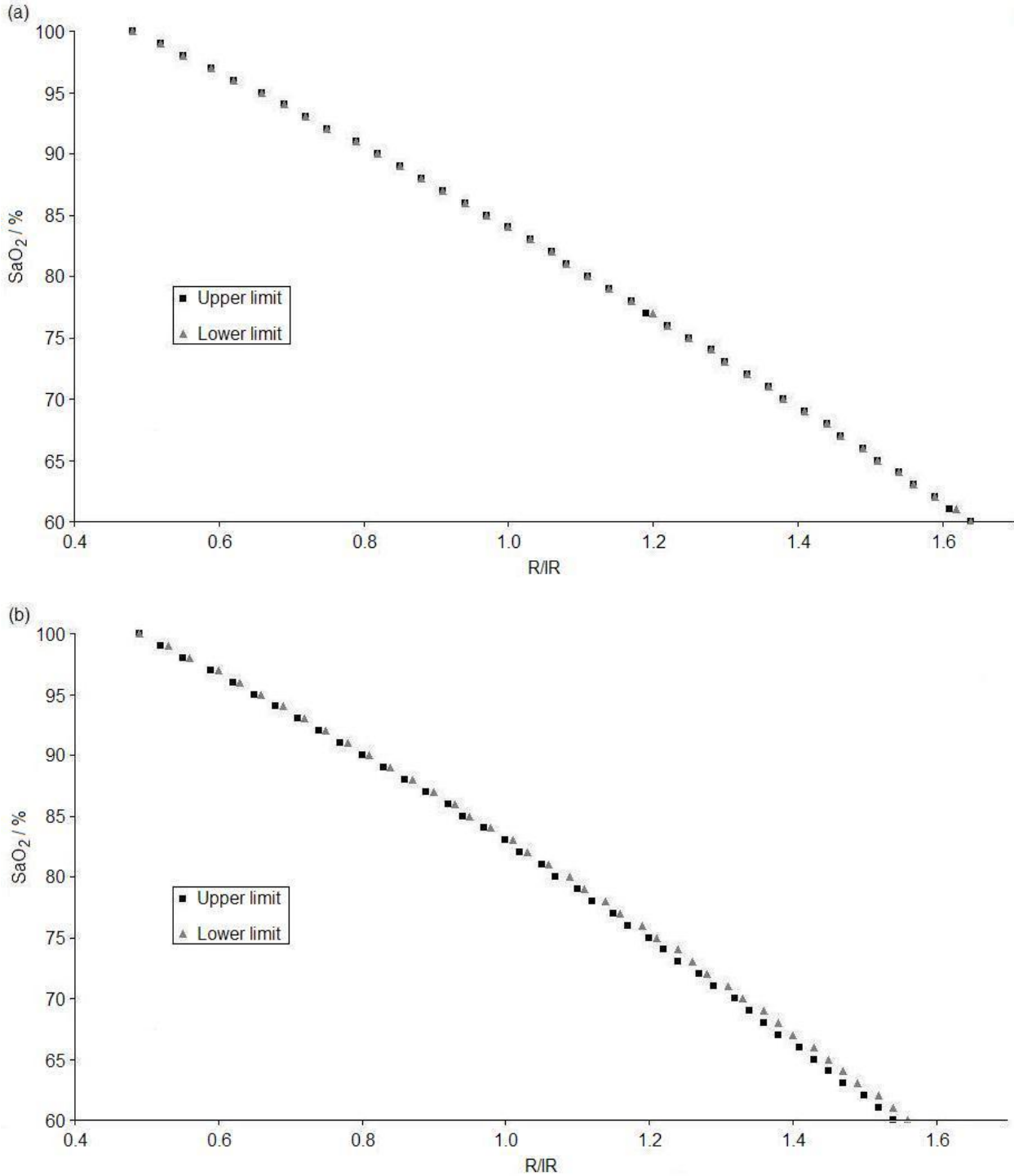


Figure 3: Pulse oximeter calibration curves generated using photon diffusion theory for the 660/940 nm pair in (a) reflection and (b) transmission mode. The shift in the curve between minimum and maximum values of  $c_g$  is especially noticeable in transmission with the largest deviations occurring at lower oxygen saturations.

$\Sigma_s$  varied by 0.31 % at 660 nm and 0.43 % at 940 nm while  $\Sigma'_s$  varied by 0.57 % and 0.56 % respectively.

For the 660/940 nm pair in transmission mode, a more significant shift in the calibration curve arose. While the shift in the curve at higher SaO<sub>2</sub> values was small (less than 1 %), an error in the pulse oximeter readout of greater than 1 % was observed below 70 % SaO<sub>2</sub> over the extremes of  $c_g$ .

## 5. CONCLUSIONS

A numerical model has been presented demonstrating the changes that occur in the bulk optical properties of arterial blood when  $c_g$  is varied over typical physiological levels. The impact that this has for pulse oximetry calibration curves has been investigated using photon diffusion theory with regard to two systems using different wavelength pairs (675/790 nm and 660/940 nm).

The variations in the bulk optical properties were small, as can be seen from figures 2 and 3, and table 3, with  $\Sigma_s$  and  $\Sigma'_s$  varying by 0.30 % and 0.57 % respectively. The change observed in  $g$  was negligible ( $< 0.01$  %). When these results were applied to the photon diffusion model, the shift in the pulse oximeter calibration curve over typical physiological variations (maximum pre/postprandial) in  $c_g$ , was clinically insignificant ( $< 1$  %) for the reflection probe set-up using 675 nm and 790 nm as source wavelengths. However, for the transmission set-up common in commercial oximeters, the changes were more significant (figure 3 (b)) – variations  $> 1$  % were observed. This is most likely because the 660/940 nm pair is more sensitive to changes in the scattering coefficients than the 675/790 pair due to the shape of the scattering spectrum – the wavelengths situated further apart have more contrasting values of  $\Sigma'_s$  associated with them and that light at these values of  $\lambda$  will experience greater changes in optical pathlength travelled. Thus, the calibration curve is more likely to be shifted as the scattering properties of the medium change. This highlights the intrinsic connection between scattering and absorption – if a photon is scattered several times in a medium, the pathlength travelled by that photon increases and the likelihood that it will be absorbed at some point increases i.e., adjusting the scattering coefficient of a turbid medium will have effects on the amount of light absorbed in that medium. This was manifested by changes in the red-to-infrared ratio in this case.

## REFERENCES

- 1 M. Kohl, M. Essenpreis and M. Cope, "The influence of glucose concentration upon the transport of light in tissue-simulating phantoms". *Phys. Med. Biol.*, 1995. **40**: p. 1267.
- 2 V. V. Tuchin, X. Xu and R. K. Wang, "Dynamic optical coherence tomography in studies of optical clearing, sedimentation, and aggregation of immersed blood". *Applied Optics*, 2002. **41**(1): p. 258-271.
- 3 J. M. Steinke and A. P. Shepherd, "Comparison of Mie theory and the light scattering of red blood cells". *Applied Optics*, 1988. **27**(19): p. 4027-4033.
- 4 C. Bohren and D. Huffman, *Absorption and Scattering of Light by Small Particles*. (Wiley-Interscience, New York, 1983).
- 5 J. M. Schmitt, F. G. Mihm and J. D. Meindl, "New methods for whole blood oximetry". *Annals of Biomedical Engineering*, 1986. **14**: p. 35-52.
- 6 V. V. Tuchin, I. L. Maksimova, D. A. Zimnyakov, et al., "Light propagation in tissues with controlled optical properties". *Journal of Biomedical Optics*, 1997. **2**(4): p. 401-417.
- 7 J. M. Schmitt, "Simple photon diffusion analysis of the effects of multiple scattering on pulse oximetry". *IEEE Transactions on Biomedical Engineering*, 1991. **38**(12): p. 1194-1203.
- 8 M. J. Leahy, *Biomedical instrumentation for monitoring microvascular blood perfusion and oxygen saturation*. 1995, Green College - University of Oxford.
- 9 C. Mätzler, *Matlab functions for Mie scattering and absorption*. (Institute of Applied Physics, Bern, 2002), <http://www.iapmw.unibe.ch/publications/pdf/files/201.pdf>. Accessed 11 August, 2004.
- 10 S. A. Prahl. (1998), <http://omlc.ogi.edu/spectra/hemoglobin/index.html>. Accessed 24 May, 2004.